Biomechanical evaluation of a novel multi-claw eyelet device for enhancing rotator cuff repair

Yiwen Zhao[1,2], Weizhe Zhang[1], Christian Tacogue[1], Xing Lei[1], Remona L Residorf[1], Wenge Ding[2], Chunfeng Zhao[1]
[1]Mayo Clinic, Rochester, MN, [2]Third Affiliated Hospital of Soochow University, The First People's Hospital of Changzhou, China
Email of Presenting Author: Zhao.Yiwen@mayo.edu

Disclosures: The authors have no COI to disclose. This work was supported by the Wendel Orthopedic Translational Research Award 2024.

INTRODUCTION: Rotator cuff tears affect 30%-50% of individuals over age 50 and are a leading cause of shoulder pain and dysfunction. Despite advances in arthroscopic techniques, postoperative retears remain common. The suture–tendon interface is consistently identified as the principal mechanical weak point, particularly in elderly patients. Multiple strategies have attempted to reinforce this interface, such as rip-stop sutures, suture tapes, and patch augmentation, which improve load sharing or biological coverage but offer inconsistent clinical benefits and increased surgical complexity. Recent suture-free and biomimetic fixation concepts, including barbed microblade patches and python-tooth–inspired devices, improve load distribution and gripping strength but may impede tendon-to-bone healing due to nonresorbable material interposition. To overcome these limitations, we developed a two-part eyelet device inspired by industrial eyelets and grommets used in textiles and footwear, aiming to redesign the contact geometry at the suture–tendon interface. (Fig. 1). Its interlocking male and female components clamp the tendon and transform localized suture stress into multiple tendon–claw contacts across a broader surface. We hypothesized that eyelet augmentation would increase failure load and construct stiffness, reduce tendon cut-through, and enhance the mechanical stability of rotator cuff repair (RCR).

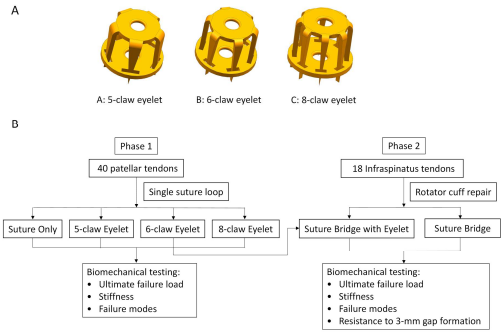

Fig. 1 (A) Design schematics showing three eyelet configurations (5-claw, 6-claw, and 8-claw). (B) Flow chart of the study design.

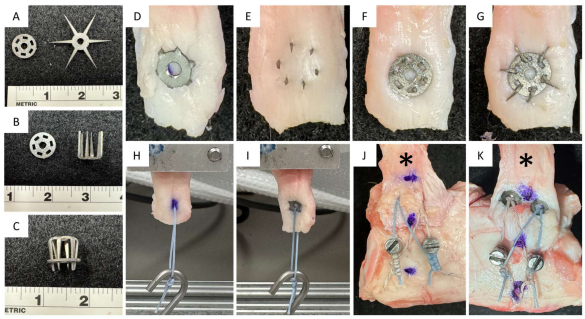

Fig. 2 (A) Original shape of the eyelet after laser cutting, with the female part on the left and the 6-claw male part on the right. (B) Each claw of the male part manually bent to 90°. (C) Assembly by inserting male claws through corresponding holes of the female part. (D) Frontal and (E) posterior views after the eyelet passes through the tendon, showing protruding claws. (F) The female part engaged on the posterior side. (G) Final configuration after bending and compressing the claws to lock both parts. (H) Porcine patellar tendon of the SO group mounted in the testing machine with the suture loop fixed to the lower hook. (I) Tendon of the eyelet group mounted in the same setup. (J) Final configuration of SB repair. (K) Final configuration of SBE repair. Asterisk (*) indicates the infraspinatus tendon (IST).

METHODS: Forty knees and eighteen shoulders were harvested from skeletally mature pigs (average body weight ≈ 44 kg) that had been sacrificed for other research purposes. No animals were euthanized specifically for this study. In Phase 1 (Single-Loop Model), forty porcine patellar tendons were randomly assigned to four groups (n = 10 each): suture only (SO) and suture with 5-, 6-, or 8-claw eyelets (5E, 6E, 8E). Eyelets were designed using CAD software and fabricated from 0.5-mm titanium alloy sheets (Fig. 2A-C). Each was mounted 10 mm from the distal tendon edge with the tendon clamped between the two components (Fig. 2D-G). Sutures (No. 2 FiberWire, Arthrex) were passed through the central hole and tied 20 mm from the distal edge with one TSOL knot followed by three square knots, forming a distal loop (Fig. 2H-I). In Phase 2 (Rotator Cuff Repair Model), nine pairs of porcine shoulders (n = 9) were prepared, preserving the infraspinatus tendon (IST). Contralateral shoulders were randomly allocated to conventional suture-bridge repair (SB) or eyelet-augmented repair (SBE). In SB repairs, two medial anchors were inserted 3 mm lateral to the articular margin at a 45° deadman's angle, and sutures were passed 12 mm from the tendon edge to create a crossed suture-bridge construct (Fig. 2J). In SBE repairs, two 6-claw eyelets were implanted 12 mm from the tendon edge, 10 mm apart, and sutures were fixed laterally in the same pattern (Fig. 2K). All constructs were mounted on a custom uniaxial tensile testing system and loaded to failure at 1.5 mm/s. Load–displacement curves were used to determine ultimate failure load, stiffness, resistance to 3-mm gap formation (measured by video tracking), and failure mode. Statistical analyses were performed using GraphPad Prism 10. One-way ANOVA was used for Phase 1 and paired t-tests for Phase 2, with significance set at $P < 0.05$.

RESULTS: In Phase 1, all eyelet groups (5E, 6E, 8E) demonstrated significantly higher failure load and stiffness than the SO group (all $P < 0.001$). Failure load was greater in 6E and 8E than in 5E ($P < 0.05$), stiffness did not differ among the eyelet groups. All specimens failed by suture or eyelet cut-through. As 6E provided comparable strength and stiffness to 8E with less variability, it was selected for Phase 2(Fig. 3A). In Phase 2, the SBE group showed 153% greater 3-mm gap resistance ($P < 0.001$), 151% higher failure load ($P < 0.001$), and 88% greater stiffness ($P < 0.05$) compared with the SB group (Fig. 3B). Predominant failure modes shifted from suture cut-through in SB (7/9) to tendon rupture in SBE (5/9).

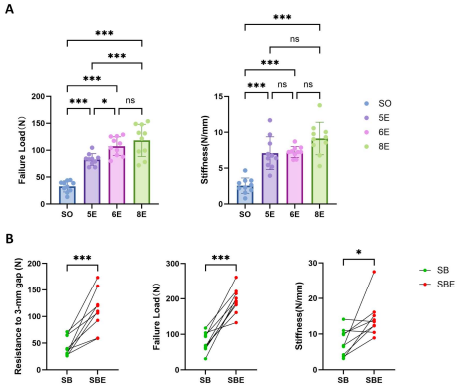

Fig. 3 (A) Phase 1: Ultimate failure load and stiffness among the SO, 5E, 6E, and 8E groups. (B) Phase 2: Resistance to 3-mm gap formation, ultimate failure load, and stiffness in rotator cuff repairs performed without (SB) or with (SBE) eyelet augmentation.

DISCUSSION: In this biomechanical study, we evaluated a novel two-part eyelet device designed to reinforce the suture–tendon interface. In Phase 1, all eyelet groups increased failure load and stiffness compared with the SO group. In Phase 2, the SBE group demonstrated significantly greater failure load, stiffness, and 3-mm gap resistance than SB, with predominant failure modes shifting from suture cut-through to tendon rupture. These findings suggest that the eyelet device enhances the initial stability and biomechanical strength of RCR. We attribute these effects to two structural features of the eyelet: (1) multiple claws redistribute stress from a focal suture point into several tendon–claw interfaces, reducing local stress concentration; (2) clamping between the male and female components generates frictional resistance once sliding begins, enhancing construct stability. This study has several limitations. First, all experiments were performed at time zero; thus, the biological aspects of rotator cuff healing could not be replicated in this model. Second, although porcine tendons offer consistency and reduce variability, they cannot fully represent the chronic degeneration seen in human tears, where the eyelet might provide even greater benefit. Third, cyclic loading was not performed, which would better simulate repetitive shoulder motion, but initial fixation strength remains a key determinant of early retear risk. Fourth, the current prototype requires manual implantation and is not yet arthroscopically applicable, though future iterations will aim to integrate the eyelet into an arthroscopic delivery system. Finally, only a metallic prototype was tested; future studies will explore biodegradable materials to enhance safety and clinical translation.

CLINICAL RELEVANCE: By redistributing stress across the suture–tendon interface, the eyelet device may offer a novel, clinically translatable strategy to enhance repair durability and reduce retears after rotator cuff repair.